Journal of Polymer Research (2019) 26:116
https://doi.org/10.1007/s10965-019-1779-4

ORIGINAL PAPER

Preparation and characterization of oxaliplatin drug delivery vehicle based on PEGylated half-generation PAMAM dendrimer

Dinh Tien Dung Nguyen[1,2] · Long Giang Bach[3] · Thi Hiep Nguyen[4] · Minh Hieu Ho[4] · Minh Nhat Ho[1,2] · Dai Hai Nguyen[1,2] · Cuu Khoa Nguyen[1,2] · Thai Thanh Hoang Thi[5]

Received: 21 December 2018 / Accepted: 8 April 2019
© The Polymer Society, Taipei 2019

Abstract

Dendrimers were well-known as a polymeric nanoparticle drug carrier system. Among them, polyamidoamine (PAMAM) dendrimers were firstly and systematically studied. Herein, to explore the additional modification of PAMAM for drug deliver application, this study assessed the PEGylated half-generation G3.5 to load oxaliplatin (OXA). The proton nuclear magnetic resonance (^{1}H NMR) and Fourier-transform infrared spectroscopy (FTIR) spectroscopy were used to confirm the successful synthesis of G3.5, and PEGylated G3.5. PEG modification on G3.5 neutralized the negative charge of G3.5 that was confirmed by zeta potential measurement, and increased the dimension of G3.5 from 10 to 100 nm that was carried out by TEM technique. G3.5-PEG showed the high drug loading efficiency of 75.69%. The release kinetic of OXA from G3.5-PEG@OXA indicated that no burst released phenomenon occurred (11.95% within first hour) and sustainable release was achieved. In cytotoxicity test with normal cells of L929 fibroblasts, the carrier system of G3.5-PEG did not induced any cytotoxicity. To test the killing effect of G3.5-PEG@OXA on cancerous cells of human cervical cancer cells (HeLa), lung adenocarcinoma (A549), and breast cancer (MCF-7), resazurin test and live/dead staining assay was used to observe the alive cells. The increase of OXA amount in G3.5-PEG@OXA lead to decrease the cell viability from 79.90–56.97% (HeLa), 84.80–64.00% (A549), and 92.00–65.00% (MCF-7) after 48 h treatment.

Keywords PAMAM dendrimers · Oxaliplatin · Drug delivery · Cancer · Nanoparticles

Introduction

Cancerous diseases is one of the causes leading to mortality in the world. In few recent decades, the development of nanotechnology have shown a great promise in cancer therapy [1]. Various types of anticancer agents including proteins, genes, hydrophilic, and hydrophobic drugs were encapsulated or conjugated in nanocarrier system in order to improve the stability, the availability, and the concentration of anticancer agents in tumor environments [1]. Magnetic and biomimetic nanoparticles, inorganic nanoparticles, liposomes, micelles, and polymeric-based nanocarriers were the main examples of nanotechnology development [2]. Although many nanomedicines were studied and even approved by the US Food and Drug Administration for cancer therapy, no one could be suitable for all clinical usages. Thus the nanocarriers has been continuously engineered to expand for many different applications.

Dinh Tien Dung Nguyen and Long Giang Bach contributed equally to this work

✉ Thai Thanh Hoang Thi
hoangthithaithanh@tdtu.edu.vn

[1] Vietnam Academy of Science and Technology, Graduate University of Science and Technology, Hanoi, Vietnam

[2] Vietnam Academy of Science and Technology, Institute of Applied Materials Science, 01 TL29 District 12, Ho Chi Minh City 70000, Vietnam

[3] Nguyen Tat Thanh University, 300A Nguyen Tat Thanh, District 4, Ho Chi Minh City 700000, Vietnam

[4] International University, Vietnam National University-Ho Chi Minh City (VNU-HCMC), Ho Chi Minh City 700000, Viet Nam

[5] Biomaterials and Nanotechnology Research Group, Faculty of Applied Sciences, Ton Duc Thang University, Ho Chi Minh City, Vietnam

Published online: 18 April 2019

Dendrimers are the third route to form the three-dimensional nanostructures. Dendrimers possess many advantages that is useful in biomedical applications, especially in drug carrier systems [3, 4]. Dendrimers have defined, monodisperse, and stable structures [5]. The dendritic architecture is similar to biological systems at the nanometer level including amylopectin, proteoglycans and glycogen to centimeter and millimeter scales such as lungs, kidney, liver and spleen [5]. Thus dendrimers achieve the ability of unique penetration and functional performance [5]. In addition, dendrimers have high amount of surface groups that are easily able to be modified to become a promising vector for gene delivery or other purposes. Among various dendritic platforms including poly(propylene imine), poly-L-lysine, melamine, poly(etherhydroxyamine), poly(esteramine) and polyglycerol, poly(amidoamine) (PAMAM) dendrimers were firstly and systematically studied. PAMAM-COOH dendrimers is an odd generation. PAMAM-NH_2 is an even generation. These peripheral groups increase exponentially following the increase of generation [3]. The rigidity of overall dendrimer structure is belong to the number of generation. The low dendrimer generation is more flexible and open, less three-dimensional shape than the high generation [3]. In biomedical applications, the choice of dendrimer generation is an important factor to compromise the unique physicochemical behavior of dendrimer as well as the loading capacity of therapeutic agents to approach an effective treatment. Although the dendrimer generation most popularly used are the fourth one or higher to exploit their full advantages [3]. In our study, dendrimer PAMAM G3.5 was utilized because the PEGylation leads to increase the G3.5 PAMAM size estimated equally the popular generation of 4.0.

PEG is a synthetic polymer possessing a high solubility in aqueous solution. It is non-toxic and non-immunogenic polymer. Thus, PEG is usually attached on protein, natural polymers, and nanocarriers for several purposes in medical applications [6, 7]. The attachment of PEG could protect the therapeutic agents from the recognition of immune systems, the degradation of enzymes, or the renal clearance of protein and peptide agents [7]. As a result, the stability and the pharmacokinetic properties of drug could be improved that leads to achieve a more effective therapy [7, 8]. Also the molecular weight of PEG should be controlled in order that the pegylated materials could not cause the deduction of biological activity due to hindrance. Herein, to form the PAMAM G3.5 dendrimer facilitating drug delivery, PEG was conjugated to G3.5 surface. Pegylated PAMAM G3.5 was studied due to these reasons that are to protect dendrimer from the detection of immunological system, and to understand the performance of pegylated G3.5.

Oxaliplatin is an anticancer drug of platinum derivative and slightly soluble in water [9]. Oxaliplatin can cause DNA lesions, inhibit DNA synthesis, and trigger the immunologic reactions in cancer cells that leads to cell apoptosis. Despite of its better tolerability in comparison with other platin compounds, oxaliplatin still remains many side effects such as nausea, diarrhea, vomiting, and/or cellular mechanisms of resistance [9]. In addition, oxaliplatin also impacts on not only the cancer cells but also the normal cells [10]. To deal with these limitations, oxaliplatin was encapsulated in pegylated PAMAM G3.5 dendrimer that is so-called G3.5-PEG@OXA to develop the new carrier system with less cytotoxicity for normal cells and less side effects. The molecular characterization of G3.5-PEG@OXA was measured using ^{1}H NMR, UV-Vis, DLS, TEM and zeta potential analyzer, respectively. Furthermore, the release kinetic of oxaliplatin from G3.5-PEG@OXA was investigated in a physiological pH of 7.2 and a lysosomal pH of 5.4 using HPLC. Finally, in vitro effects of G3.5-PEG@OXA on normal and cancer cells were explored using resazurin and live/dead tests.

Experimental

Materials

Poly(ethylene glycol) (PEG, molecular weight = 4000 Da), 4-dimethylamino pyridine (DMAP), and p-nitrophenylchloroformate (PNC) were purchased from Sigma Aldrich (St Louis, MO, USA). Triethylamine (TEA) was supplied by KANTO CHEMICAL Corp. (Tokyo, Japan). Aluminum oxide was bought from Strem Chemical Inc. (Newburyport, MA, USA). Ethylene diamine (EDA), methyl acrylate (MA), 1-ethyl-3-(3-dimethylaminopropyl) carbodiimide (EDC, 97%) and *N*-hydroxysuccinimide (NHS, 98%) were obtained from Merck (Darmstadt, Germany). Dialysis membrane with MWCO of 3500 Da was bought from Spectra/Por® (TX, USA).

Oxaliplatin European Pharmacopoeia (EP) Reference Standard (OXA, [SP-4-2-(1R-trans)]-(1,2-cyclohexanediamine-N,N′)[ethanedioata(2–)-O,O′]platinum, >98.0%, M_w 397.29 g/mol) was bought from Sigma-Aldrich (is now Merck, St Louis, MO, USA).

For the cell study, Dulbecco's modified Eagle medium (DMEM), penicillin−streptomycin (P/S), and trypsin/EDTA were purchased from Gibco BRL (Grand Island, NY, USA). Fetal bovine serum (FBS) and Dulbecco's phosphate buffered saline (DPBS) were purchased from Wisent (Saint-Bruno, QC, Canada). Resazurin sodium salt was obtained from Sigma-Aldrich (Merck, St Louis, MO, USA). Other chemicals and solvents were used without further purification.

Synthesis of aminated-PEG (PEG-NH_2)

PEG-NH_2 was synthesized by a two-step reaction including the activation of terminal alcohols for the formation of carbonates in the presence of DMAP and the coupling between

carbonates and nucleophilic component [11]. In brief, purified mPEG (0.16 mmol) was added into the round flask under vacuum at 65 °C. After 1 h, PNC (0.19 mmol) was added into mPEG. The reaction between mPEG and PNC was carried out for 6 h. Then the reaction temperature was gone down to 40 °C. Tetrahydrofuran (20 mL) was added into the reaction flask to dissolve completely all chemical mixture. The obtained solution was added dropwise into another round flask containing 20 μL of EDA. This reaction was performed at room temperature (RT) for 24 h under stirring condition. After that, the reacted solution was added into the beaker containing 500 mL of diethyl ether in order to precipitate the mPEG-NH_2. The precipitation of mPEG-NH_2 was filtered by vacuum-pump and was then dried under vacuum at RT. The dried mPEG-NH_2 was light yellow powder. To confirm the successful amination of mPEG, ^{1}H NMR (Bruker AC 500 MHz spectrometer, Bruker Co., Billerica, MA, USA) was utilized.

Synthesis of PAMAM dendrimer G3.5 grafted mPEG (G3.5-PEG)

PAMAM dendrimers were synthesized from the repeating steps of Michael addition reaction and amidation one as previously we reported [11]. In this study, PAMAM dendrimers of generation 3.5 (G3.5) was utilized. First, MA of 40 mL was added into the round flask containing methanol of 40 mL, the temperature was adjusted to 0 °C using ice bath. After stirring homogenously, EDA of 5.5 mL was dropped into MA solution. The temperature of 0 °C was maintained to perform the reaction for 3 h. Then increasing the temperature to RT, the reaction was continued for 2 days. The reaction mixture was connected to the rotary evaporator (Strike 300, Lancashire, PR6 0RA, UK) to remove methanol and unreacted MA, the obtained products was the dendrimer core precursor. To continue the step-growth of dendrimers, the core precursor of 20 g was dissolved in 10 mL of methanol. This solution was then added into the round flask containing 130 mL of EDA. The temperature was kept at 0 °C for 3 h. After that, the reaction was continuously carried out at RT for 4 days. To remove the EDA residues and solvents, the reacted solution was added a toluene/methanol (9/1 *v*/v) mixture, then connected with the rotary evaporator. The temperature of water bath was kept at 45 °C. To remove the excess toluene, methanol was added and performed the similarly rotary evaporation program. The purified product was dendrimer generation of 0.0 (G0.0). To obtain dendrimer generation of 3.5, those couple steps were repeated continuously 3 times plus the step of Michael addition reaction. 1H NMR spectrometer was utilized to confirm the successful synthesis of G3.5 (in solvent of D_2O).

Generation 3.5 PAMAM dendrimer was modified with PEG-NH_2 using EDC/NHS to create G3.5-PEG. By varying PEG-NH_2 amount, different PEGylation degrees of G3.5-PEG was obtained. Then, ^{1}H NMR and FT-IR were used to confirm their structure.

Gel permeation chromatography (Agilent GPC/SEC 1100, CA, USA) was performed to determine the average molecular weights of G3.5 and G3.5-PEG. GPC system was equipped with 1260 infinity II manual injector, 120 Ultrahydrogel column (300 mm × 7.5 mm, 10 μm, Waters, MA, USA), and an Optilab DSP interferometric refractometer (Wyatt Technology Co.). The mobile phase was 0.1 M $NaNO_3$ aqueous solution. A flow rate passing through the column was 1 mL/min. The sample volume of G3.5 or G3.5-PEG for manual injection was 100 μL. The temperature of detector and column was 35 °C. A series of PEG standards (Waters, MA, USA) were used to calculate the M_w.

Drug encapsulation and in vitro drug release profile

OXA was dissolved completely in DI water of 5 mL in glass bottle A and stirred homogenously for 1 h. In glass bottle B, G3.5-PEG was dissolved in DI water of 10 mL and stirred for 10 min. After that, OXA solution was poured gradually into G3.5-PEG solution. The mixture was then stirred carefully for 24 h at RT to form G3.5-PEG encapsulating OXA (G3.5-PEG@OXA). After that, whole mixture solution was poured into the dialysis tube with MWCO 3500 Da, DI water of 25 mL was used to dialyze for 1 h. DI water was exchanged 4 times every hour. The exchanged DI water was collected to determine the free OXA using HPLC (Perkin Elmer Flexar). The mixture inside dialysis tube after dialysis was lyophilized to obtain the dried G3.5-PEG@OXA.

The drug loading efficiency (DLE) were calculated according to the following equations:

$$\mathrm{DLE} = \frac{m_o^{OXA}}{m_1^{OXA}} \times 100\% \quad (1)$$

m_o^{OXA} weight of OXA in G3.5-PEG carrier
m_1^{OXA} mass of OXA in feed

To explore the OXA release profile from G3.5-PEG@OXA system, dialysis procedure and HPLC technique was used. In detail, the dried G3.5-PEG@OXA of 5.0 mg was dissolved in DI water of 2500 mL to prepare the G3.5-PEG@OXA solution that was transferred into dialysis tube of MWCO 3500 Da. The dialysis tube containing G3.5-PEG@OXA solution was put into the volumetric cyclinder containing 7500 mL of DPBS. The stirring mode was applied at velocity of 50 rpm. After specific time intervals of 1, 3, 6, 12 and 24 h, DPBS (pH 7.2) of 1000 mL was sampling and fresh one was added into the cyclinder. In order to investigate the

release profile of G3.5-PEG@OXA in the acidic media, the experiments were carried out similarly, but the DPBS (pH 7.2) was replaced by phosphate buffer pH 5.4. The sample solution was determined by HPLC to quantify the released OXA amount with UV detector. Methanol/HPLC-grade water (50/50 *v*/v) was used as a mobile phase. Manual injection was operated to load 100 μL of sample into the chromatography column of CAPCELL PACK C18 column (5 μm, 4.6 × 150 mm, Shiseido Co., Ltd., Tokyo, Japan). The flow rate was set up at 1 mL/min. Peaks of OXA appeared at 1.9 min. The OXA amount was calculated from the standard curve built by plotting the areas against the known concentrations. The measurement was carried out 3 times to define the standard deviation. Also OXA was encapsulated in G3.5 to form G3.5@OXA similarly to method of G3.5-PEG@OXA fabrication. The release test of G3.5@OXA in the media pH of 5.4 and 7.2 was performed as the same with G3.5-PEG@OXA for comparison.

Cell compatibility and cytotoxicity test

Cell compatibility test with L929

To evaluate the cell compatibility of materials not encapsulated OXA, fibroblast L929 cell line was used to contact with G3.5 and G3.5-PEG solution, and the control of cell medium. The sample solutions was prepared at the concentration of 1 mg/mL in Eppendorf tubes. All tubes were vortexed for 1 min at velocity of 2000 rpm, and was then put in an ultrasonic bath at 37 °C for 20 min. Those tubes were kept overnight in an incubator at 37 °C, relative humidity of 98% and CO_2 of 5%. After 1 day, the sample solution was diluted into 500 and 250 μg/mL with cell media (DMEM), followed by overnight incubation at 37 °C, relative humidity of 98% and CO_2 of 5%. The L929 cells (1.5×10^5 cells/mL, 100 μL) were seeded in 96-well plate. The cell media was the DMEM mixing with 10% of FBS and 1% of PS, which is shortly called the cell media of DMEM. After 1 day for full spreading, the cell media was removed, the

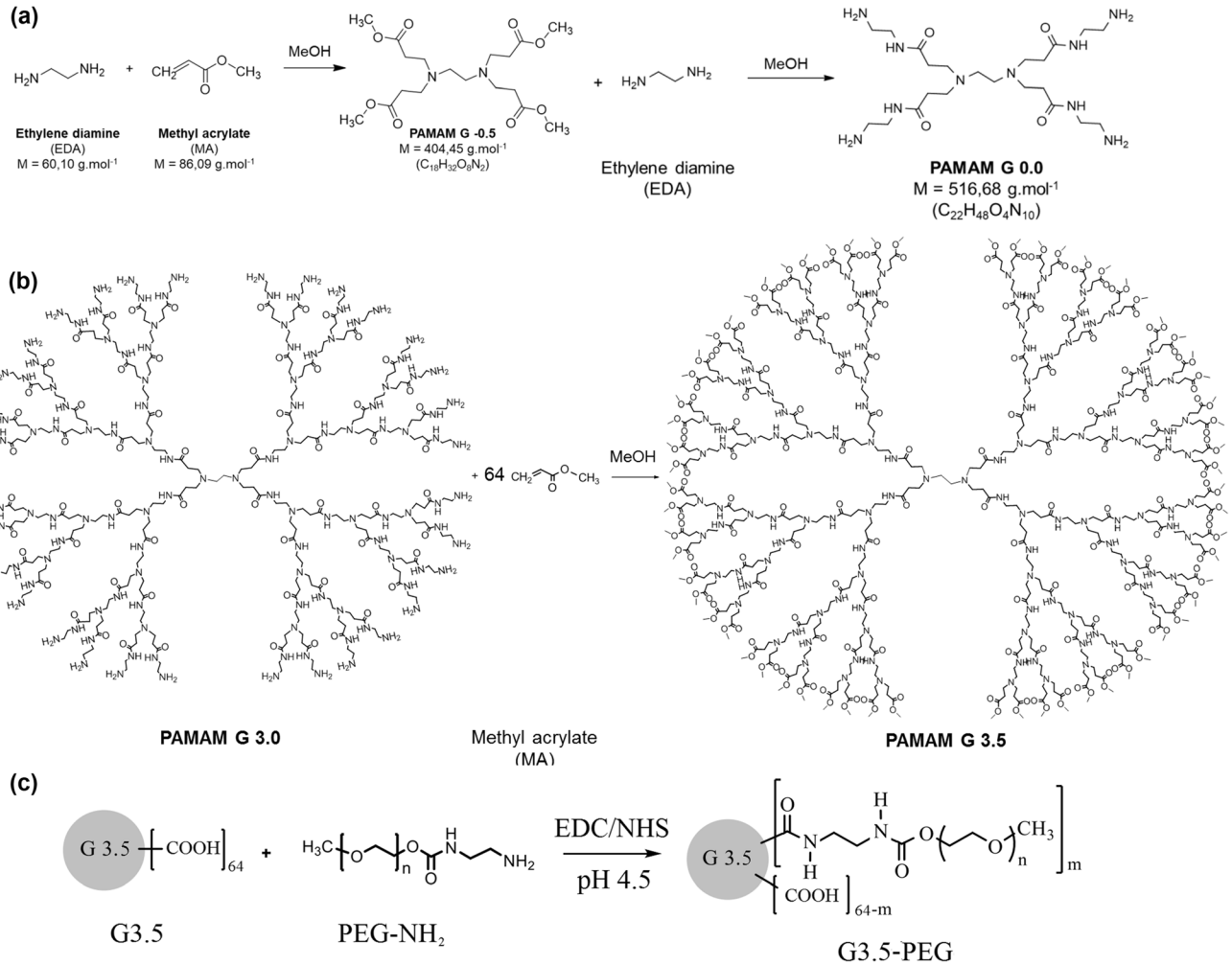

Fig. 1 Synthesis scheme of PAMAM G3.5 (**a**, **b**) and the modification reaction of PEG-NH_2 on PAMAM dendrimer G3.5 surface to create G3.5-PEG (**c**)

sample solution was added to contact the L929 cells. Each sample was repeated three times for three wells. After 24 h and 48 h, the cell media was removed and filled with 10 μL of resazurin solution (0.2 mg/mL). All cells were incubated for 4 h in an incubator. To determine qualitatively cell viability, after incubating with resazurin, 100 μL of cell media of each well was read by microplate reader at excitation/emission of 560/590 nm. The images of cells were observed by fluorescence microscopy (TE2000, Nikon, Japan).

Cytotoxicity of G3.5-PEG@OXA system using Hela, A549 and MCF-7 cells

The G3.5-PEG@OXA amount was calculated to have enough 1 mg of OXA. All samples was weighed into Eppendorf tubes, adjusting the volume of cell media added was to obtain the concentration of 1 mg/mL. The tubes were vortexed for 1 min at 2000 rpm, and were then put into the ultrasonic bath at 37 °C for 20 min. The incubation of those tubes were carried out overnight at 37 °C, relative humidity of 98% and CO_2 of 5%. After 1 day, the samples were diluted into 100, 75, 25, and 10 μg/mL with cell media, and were then incubated overnight at 37 °C, relative humidity of 98% and CO_2 of 5%. Those sample solutions were utilized to treat Hela, A549 and MCF-7 cells seeded in 96-well plate as the similar way described for L929 cells. To determine qualitatively Hela, A549 and MCF-7 cell viability, resazurin solution was used as the similar procedure with L929 cells. The images of cells were observed by fluorescence microscopy (TE2000, Nikon, Japan).

To observe the morphology of L929, Hela, A549 and MCF-7 cells, fluorescein diacetate (FDA) of 10 mM and ethidium bromide (EB) of 7.5 mM were used to stain the cells. Those cells were incubated with 25 μL of staining reagents for 3 min at 37 °C under 5% CO_2 atmosphere in dark condition. Fluorescence microscopy (TE2000, Nikon, Japan) was operated to examine the cell morphology.

Statistical analysis

All data are presented as means ± standard errors. Statistical analyses were performed using Student's t test. A P value smaller than 0.05 was considered statistically significant.

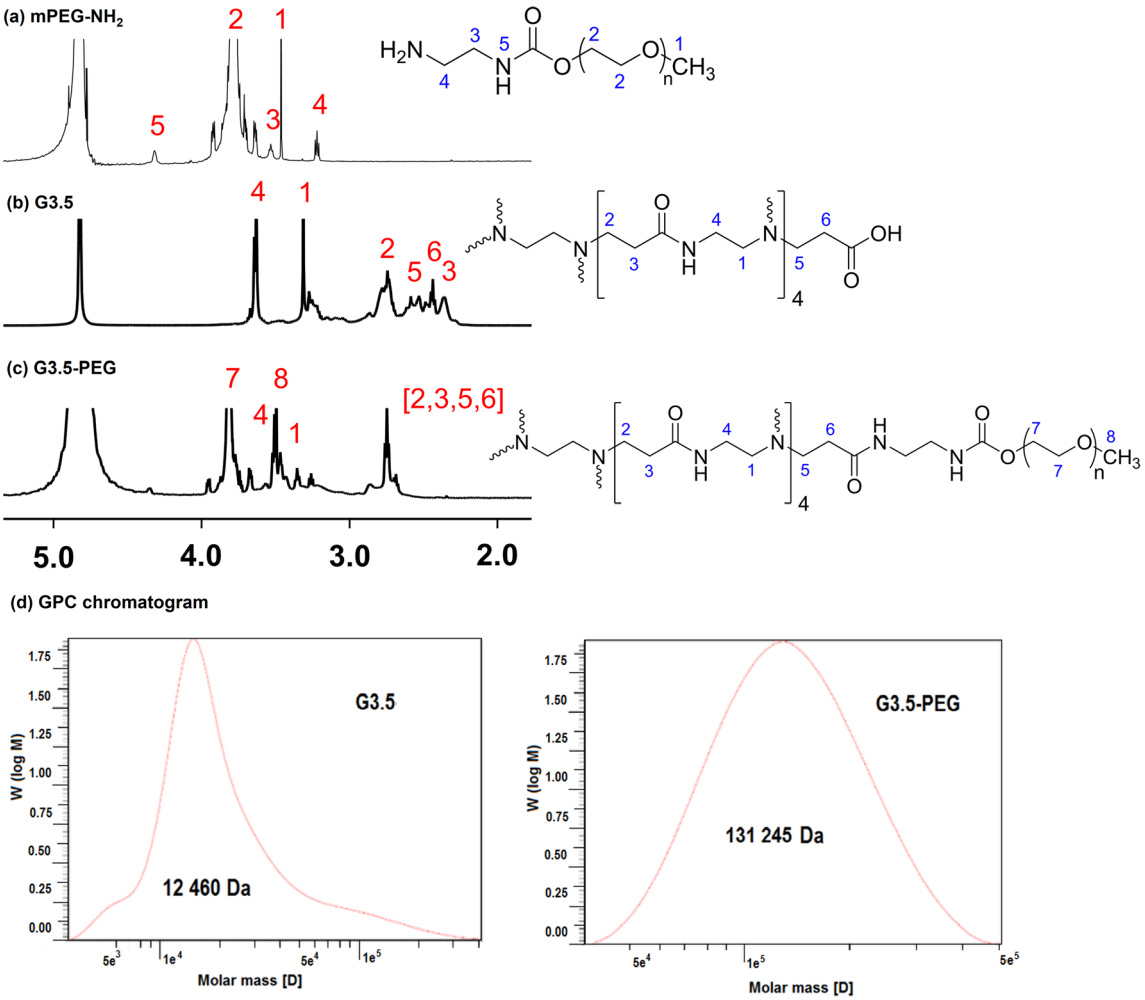

Fig. 2 ^{1}H NMR spectra (500 MHz, 298 K) of (**a**) PEG-NH_2, (**b**) PAMAM dendrimer G3.5, (**c**) in D_2O. GPC chromatograms of G3.5 and G3.5-PEG (d)

Results and discussion

Synthesis of PAMAM dendrimer G3.5 grafted mPEG (G3.5-PEG)

PAMAM G3.5 dendrimer was synthesized following a divergent route [3]. Ethylenediamine was a core site to start the synthesis procedure. A dendrimer was grown up by using methyl acrylate (MA) to attach on amine groups of a core site through Michael reaction. The double bond of MA reacted with amine groups to form amine bonds (Fig. 1a). Continuously, ethylenediamine reacted with terminal carbonyl groups of MA through electrophile mechanism to form amide bonds. At the end of this step, obtained dendrimer was the zero generation. Two these couple reactions were repeated 3 times to create PAMAM dendrimer of the third generation (G3.0). Then to obtain PAMAM dendrimer of 3.5 generation, an excessive amount of MA was used to react with G3.0 completely. Herein, the amide groups were chosen as linkages for dendrimer synthesis and modification because this covalent bonding can be protonated inside the tumor to internalize the dendrimer carrier system from the antibody [12].

To confirm the structure of PAMAM dendrimer G3.5, ^{1}H NMR and FT-IR were utilized. In the Fig. 2, ^{1}H NMR spectra of PEG-NH_2, PAMAM dendrimer G3.5 and G3.5-PEG were showed. The singlet peak at chemical shift δ of 3.631 ppm was attributed to proton of methyl ended groups -O-C**H**$_3$ of PEG-NH_2 (labelled 1, Fig. 2a(i)) and G3.5-PEG (labelled 8, Fig. 2a(iii)). In addition, the other protons including the peak of 3.751–3.868 ppm (labelled 2 and in Fig. 2a(i) and 2a(ii) respectively) assigning to -C**H**$_2$-C**H**$_2$-O- groups on PEG-NH_2 backbones. These H types were not presented in G3.5 structure. This fact revealed that G3.5 was grafted successfully with PEG-NH_2 to form G3.5-PEG.

Figure 3 showed the FT-IR spectrum of PEG-NH_2, PAMAM dendrimer G3.5 and G3.5-PEG. Within the PEG-NH_2 spectrum (Fig. 3c), the appearance of peak at 2989 cm^{-1} indicated the C-H stretching vibration [13]. The peak at 1105 cm^{-1} was the C-O-C asymmetric stretch, the one at 843 cm^{-1} was the symmetric C-C-O stretch. Importantly, the strong peak at around 3300 cm^{-1} exhibiting for O-H stretch wasn't found in the PEG-NH_2 IR spectrum, but the small shoulder of the peak at 3419 cm^{-1} assigning for N-H stretch was appeared. This fact meaning all hydroxyl groups of PEG was replaced by amine that implied the successful amination of PEG. In IR spectra of G3.5 (Fig. 3b), a small shoulder around wavelength of 3500 cm^{-1} was attributed to OH bonds of carboxylic groups. A peak of 3270 cm^{-1} indicated the N-H stretching vibration of amides. The peak of 1727 cm^{-1} was C=O stretch of carbonyl groups, the peak of 1648 cm^{-1} was assigned to C=O stretch of amide groups, and two peaks are overlapped. A peak of 1360 cm^{-1} was C-N bonds of amines and amides. N-H wagging was appeared at 696 cm^{-1}. Altogether, those functional groups found by FTIR spectra was

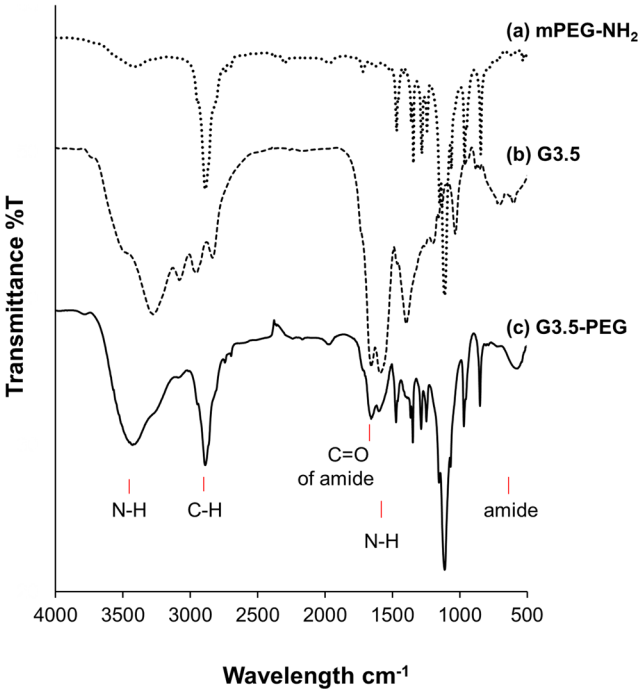

Fig. 3 FT-IR spectra of PEG with amine terminal group (**a** mPEG-NH_2), dendrimer PAMAM G3.5 (**b** G3.5), and dendrimer PAMAM G3.5 conjugated PEG-NH_2 (**c** G3.5-PEG)

consistent with PAMAM G3.5 formula that demonstrates the successful synthesis of G3.5. In IR spectrum of G3.5-PEG-NH_2, a strong peak of 3419 cm^{-1} assigning for N-H stretch indicated the terminal amine groups, the C-H stretching, the C=O stretch of amides, and N-H wagging was also found. These results revealed that PEG-NH_2 was grafted on to PAMAM G3.5 through amide links.

In addition, GPC technique was used to obtain the molecular weight M_w of G3.5 and G3.5-PEG. Figure 2 d indicated the GPC chromatogram of G3.5 and G3.5-PEG with their molecular weights of 12,460 Da and 131,245 Da respectively. The M_w of G3.5 determined by GPC was approximated to theory that confirmed G3.5 was synthesized successfully. The M_w of G3.5-PEG was 10.5-fold higher than M_w of G3.5 that also demonstrated the successful conjugation of PEG on G3.5. To calculate the number of PEG attached on G3.5 surface, the following Eq. (2) was utilized.

$$\text{Number of conjugated PEG} = \frac{M_w^{G3.5-PEG} - M_w^{G3.5}}{M_w^{PEG}} \quad (2)$$

Result showed that about 30 of PEG chains were attached on the G3.5 surface. As a result, it was approximately 47% of reacted carboxylic functional groups on G3.5 surface.

Morphological, particle size characterization

SEM images was utilized to observe the morphology of dendrimers as well as to calculate their sizes. The SEM

observation revealed that G3.5 (Fig. 4a), G3.5-PEG (Fig. 4c), and G3.5-PEG@OXA (Fig. 5a) were appeared in a particle shape. The G3.5-PEG (Fig. 4b) showed bigger particle size as comparing with unmodified G3.5 (Fig. 4b) that was consisted with the study of Zhu et al. [14]. After loading OXA, the particle size was increased to 60 nm (Fig. 5b) which is larger

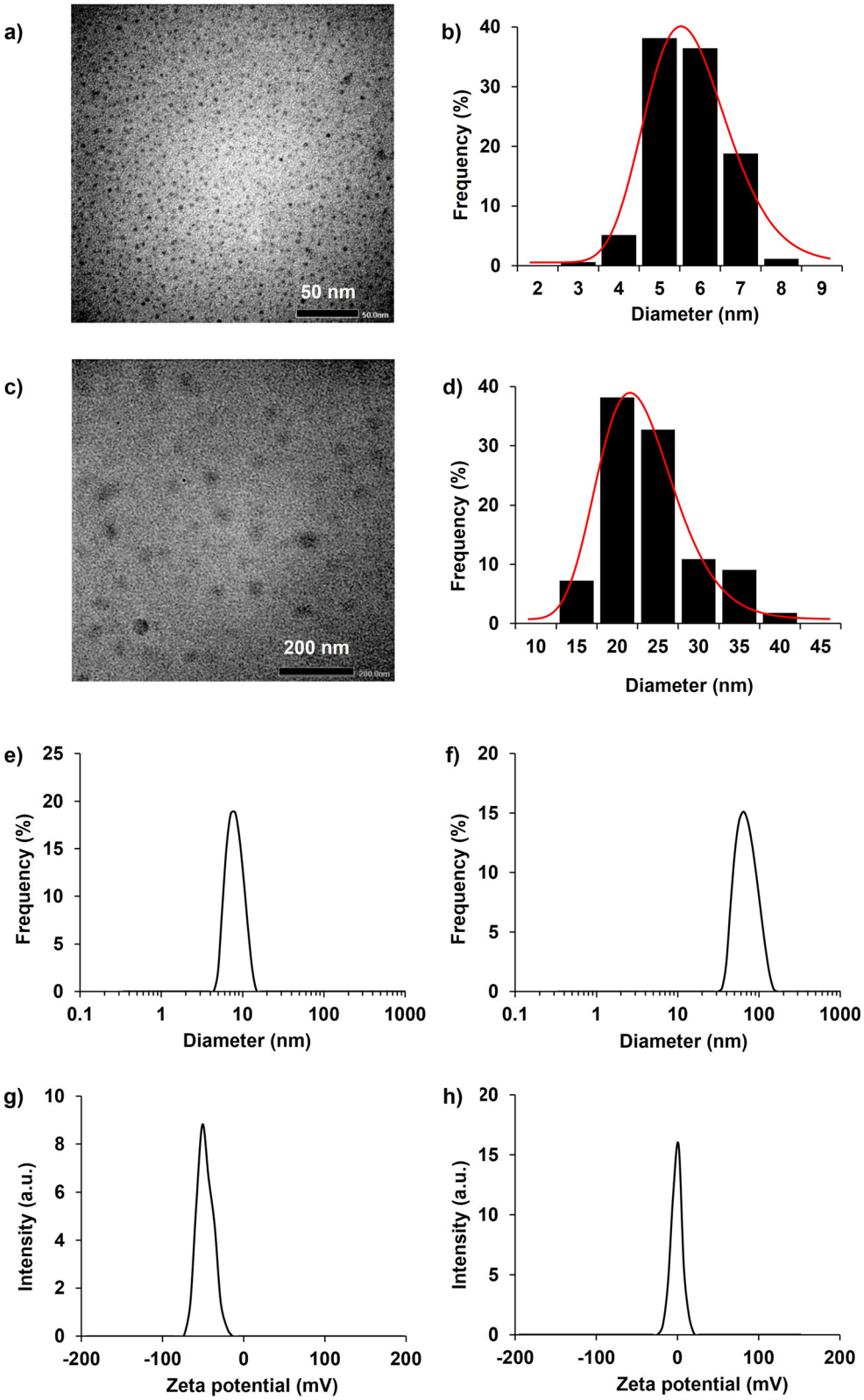

Fig. 4 Transmission electron microscopy (TEM) images of G3.5 (**a**) and its particle size distribution (**b**). TEM images of G3.5-PEG (**c**) and its particle size distribution (**d**). Determination of the hydrodynamic average diameter of G3.5 (**e**) and G3.5-PEG (**f**) by dynamic light scattering (DLS). The surface charges of G3.5 (g) and G3.5-PEG (**h**) were investigated by zeta potential analyzer

than bare G3.5-PEG. DLS measurement was also carried out to define the hydrated sizes of G3.5 and G3.5-PEG. The G3.5 and G3.5-PEG appeared around 10 nm (Fig. 4e) and 100 nm (Fig. 4f) respectively. Those sizes were higher than that calculated by SEM observation due to the hydration in aqueous solution. Especially, the hydrodynamic size of G3.5-PEG was significantly increased when compared to that of G3.5 due to the flexible PEG molecular which is able to strongly bind to water through hydrogen bond. Taking into account the aforementioned methods determining particle size, the PEGylation was confirmed that it increased the size of G3.5 dendrimer. The size of carrier system was less than 100 nm that is still sufficient to penetrate into cancerous cells.

In Figs. 4g, h and 5c, the zeta potential of G3.5, G3.5-PEG and G3.5-PEG@OXA were exhibited. The PEGylation and the encapsulation of OXA into G3.5 achieving approximately 0 mV was higher than the zeta potential of G3.5 recorded about – 40 mV. The negative potential of G3.5 implied that a terminal carboxylic group was ionized in aqueous media. The anionic G3.5 PAMAM dendrimers were reported that it is not good to cross the epithelial barriers [15]. After PEGylation, G3.5-PEG become uncharged dendrimers that can improve the OXA absorption inside tissues when compared to negative ones [15]. In addition, uncharged dendrimers was claimed that they could extend blood residence times and avoid filtration of kidney [15]. Therefore, the G3.5-PEG was as a new disposition of G3.5 to overcome the disadvantages of anionic dendrimers.

OXA encapsulation and release kinetic

In this study, OXA was utilized as a model drug to evaluate the potential ability of G3.5-PEG in drug loading and release. The OXA was immersed in G3.5 or G3.5-PEG solution, OXA physically diffused in the interior. The hydrogen bonding between OXA and dendrimer branches might occur to form the OXA encapsulated G3.5 or G3.5-PEG system [16]. In addition, the residue carboxylic groups of G3.5 or G3.5-PEG surface could interact with platinum center of OXA through coordinating bonds or ionic interactions [17]. The DLE which are the important parameter of nanomedicines was calculated and the value was 75.69 ± 8.90%. The DLE was high that shows the effective utilization of feeding amount of OXA in the loading preparation process. Also the high DLE was obtained and may be necessary for effective drug carrier.

Then the OXA-released profile at physiological pH of 7.2 and lysosomal pH of 5.4 at 37 °C was obtained through the released OXA determination as a function of time intervals. The OXA quantification was measured by HPLC and calculated from the standard curve of known OXA concentrations. Free OXA was utilized as comparison sample. OXA has high solubility in aqueous solution (7.9 mg/mL) [18] that leads to fast release of 50% of initial amount within first hour. Although OXA is a third generation of platinum-based anticancer drugs with less cytotoxicity than other ones, it still remains the side effects including peripheral distal neurotoxicity, acute dysthesias, myelosupression, etc. [12] which have

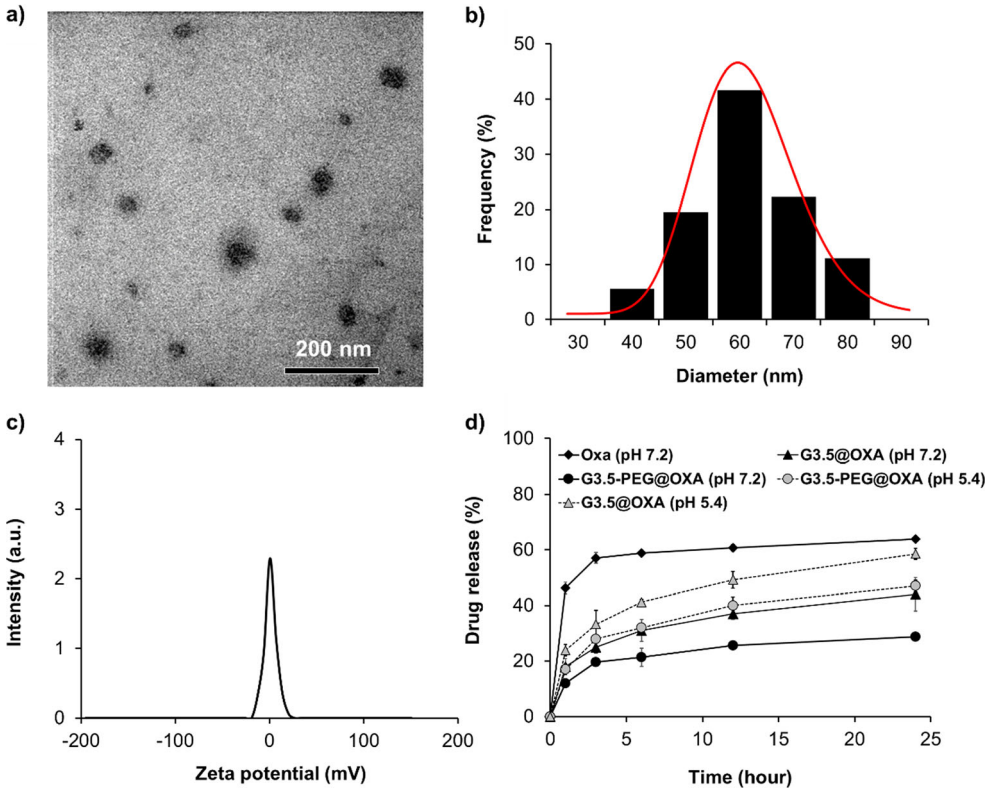

Fig. 5 Transmission electron microscopy (TEM) images of G3.5-PEG@OXA (**a**) and its particle size distribution (**b**). The surface charges of G3.5-PEG@OXA (**c**) was performed by zeta potential analyzer. The released OXA amount of free OXA, G3.5@OXA and G3.5-PEG@OXA in phosphate buffer pH of 7.2 and 5.4 was determined by HPLC (**d**)

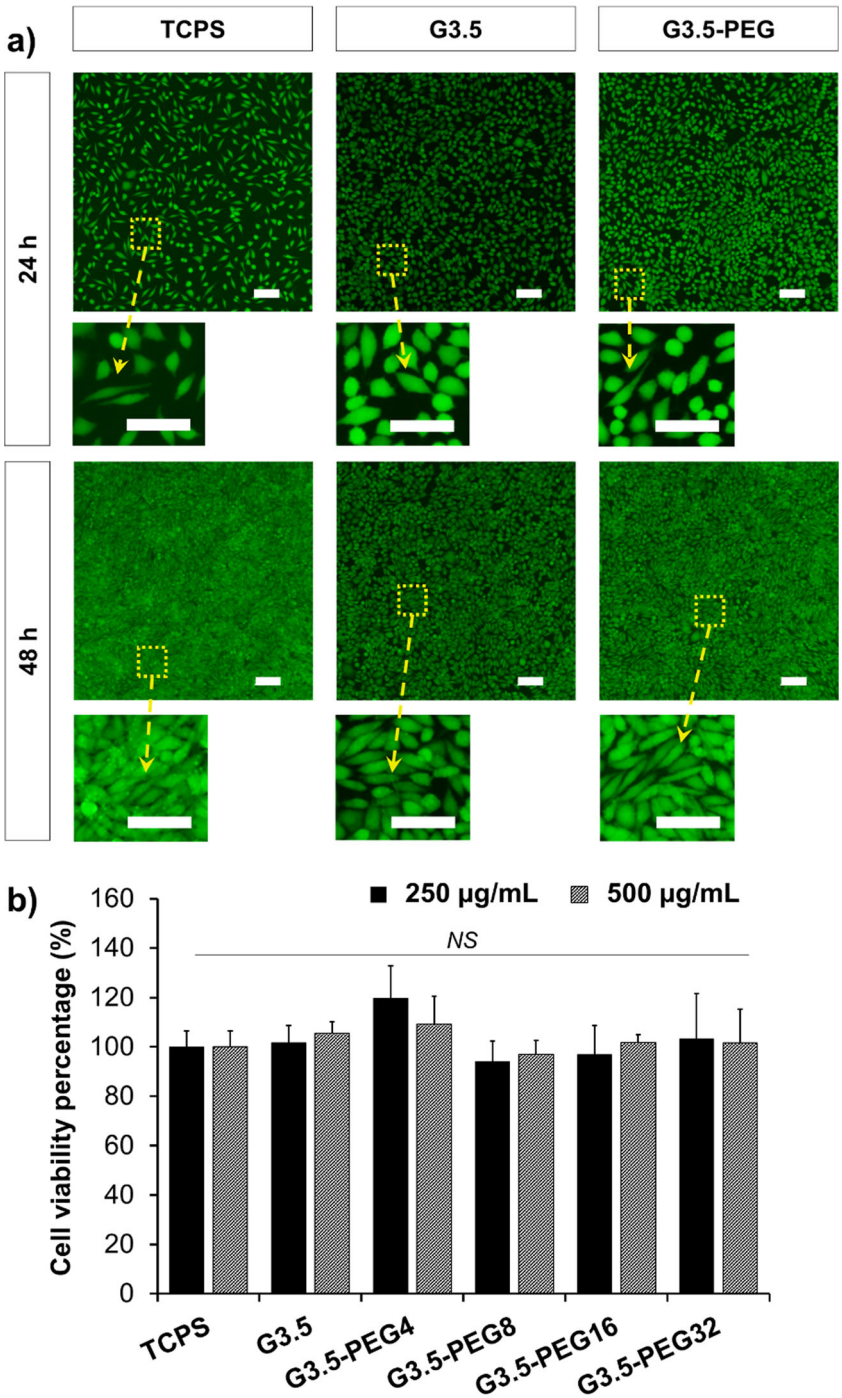

Fig. 6 Fluorescence microscopy images of FDA/EB stained L929 fibroblasts after contacting G3.5 and G3.5-PEG solution (500 μg/mL) within 24 h and 48 h (**a**). L929 viability percentage was calculated by using the OD data measured with resazurin assay. L929 was incubated with G3.5, G3.5-PEG4, G3.5-PEG8, G3.5-PEG16, and G3.5-PEG32 at material concentrations of 250 and 500 μg/mL. L929 in the cell media (named as TCPS) was a control (**b**). Scale bar: 100 μm. *NS*: non-statistical difference

to be prevented. Thus G3.5@OXA and G3.5-PEG@OXA were studied to explore the released kinetic that is necessary. At the pH 7.2, the released OXA from G3.5@OXA was slower than OXA free about 2.5-fold at first hour, 2.3-fold at third hour, and 1.4-fold at 24th hour (1 day). The released amount of OXA in G3.5-PEG@OXA was 3.9-fold lower than free OXA at first hour, 2.9-fold at the third hour and 2.2-fold at 24th hour (1 day). These results indicated that G3.5 and G3.5-PEG can decrease the released OXA amount to overcome the burst release phenomenon of free OXA at the physiological pH of 7.2. Also, it was recognized that the released OXA amount from G3.5 was higher than that from G3.5-PEG. It might be due to the PEGylation of G3.5 surface hindering the diffusion of OXA from the nanoparticle core to solution. The utilization of G3.5-PEG supported to overcome the burst release of free OXA and then to prolong the release time of encapsulated OXA. In fact, Fig. 5d indicated the sustained release property of G3.5-PEG up to 24 h. When performing the release test of G3.5@OXA and G3.5-PEG@OXA in the acidic media, the released OXA amounts were higher 1.33-

and 1.63-fold respectively than that in the pH of 7.2. This evidence could be explained by the pH-dependent conformational behavior of dendrimers [19, 20]. PAMAM dendrimers can be protonated at the tertiary amines within their core and branches at lower pH [3, 19, 21]. Thus the electrostatic repulsion appeared among the dendrimer branches that leads to increase OXA release. This enhancement of released OXA in the pH of 5.4 may reduce the side effects of OXA and increase its bioavailability to cancerous sites. Although the released OXA amount from G3.5-PEG@OXA was lower than G3.5@OXA due to the PEG shell, G3.5-PEG@OXA possessed less negative charge of carboxylic groups than G3.5@OXA that are more favourable to interact with biological membranes to permeate across epithelial barriers [19, 22].

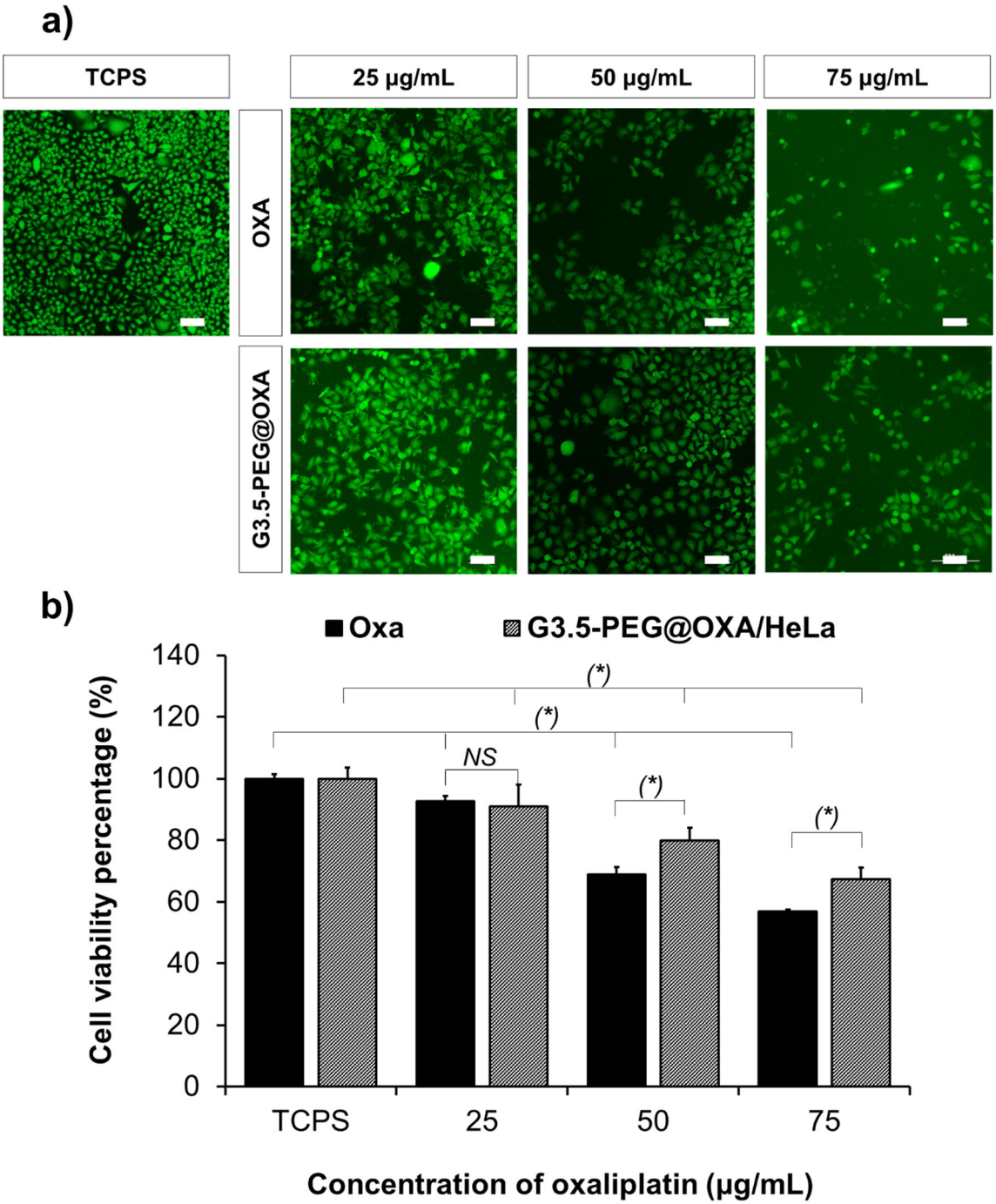

Fig. 7 HeLa cells were incubated with free OXA and G3.5-PEG@OXA at various OXA concentrations for 48 h, and in the cell media (named as TCPS - a control). Then HeLa cells were stained by FDA/EB and observed by fluorescence microscopy (**a**). HeLa viability percentage was calculated by using the OD data measured with resazurin assay (**b**). Scale bar: 100 μm. (*) $P < 0.05$, *NS*: non-statistical difference

Evaluation of biocompatibility

To demonstrate the non-toxic property of carrier system, the G3.5 and PEGylation of G3.5 with various PEG content were tested with fibroblast L929. After culturing the fibroblast L929 on TCPS, when all cells attached and spead almost 100% of well surface, the media mixed with G3.5 and G3.5-PEG solution of 250 and 500 μg/mL was added into each well. The fibroblast L929 was cultured with only media that was used as a control sample. After 24 h and 48 h, the fibroblast L929 contacting carrier materials was stained with live/dead assay to observe cell morphology, and was quantified the viability using resazurin reagent. Figure 6a showed that almost fibroblasts L929 were alive after contacting G3.5 and G3.5-PEG for 24 h as well as 48 h. The cell morphology in G3.5 and G3.5-PEG well were not different from the control, they changed their shape obviously from round to elongation and achieved the high density of cells. Figure 6b indicated the quantitative viability of fibroblasts L929 on each sample. Both the cells in contact with G3.5 and G3.5-PEG achieved the high viability of around 100% when compared to the cells without treatment. Those results confirmed that the G3.5 and G3.5-PEG were not toxic to fibroblasts L929. In fact, G3.5 with terminal carboxylic groups were reported as non-toxic

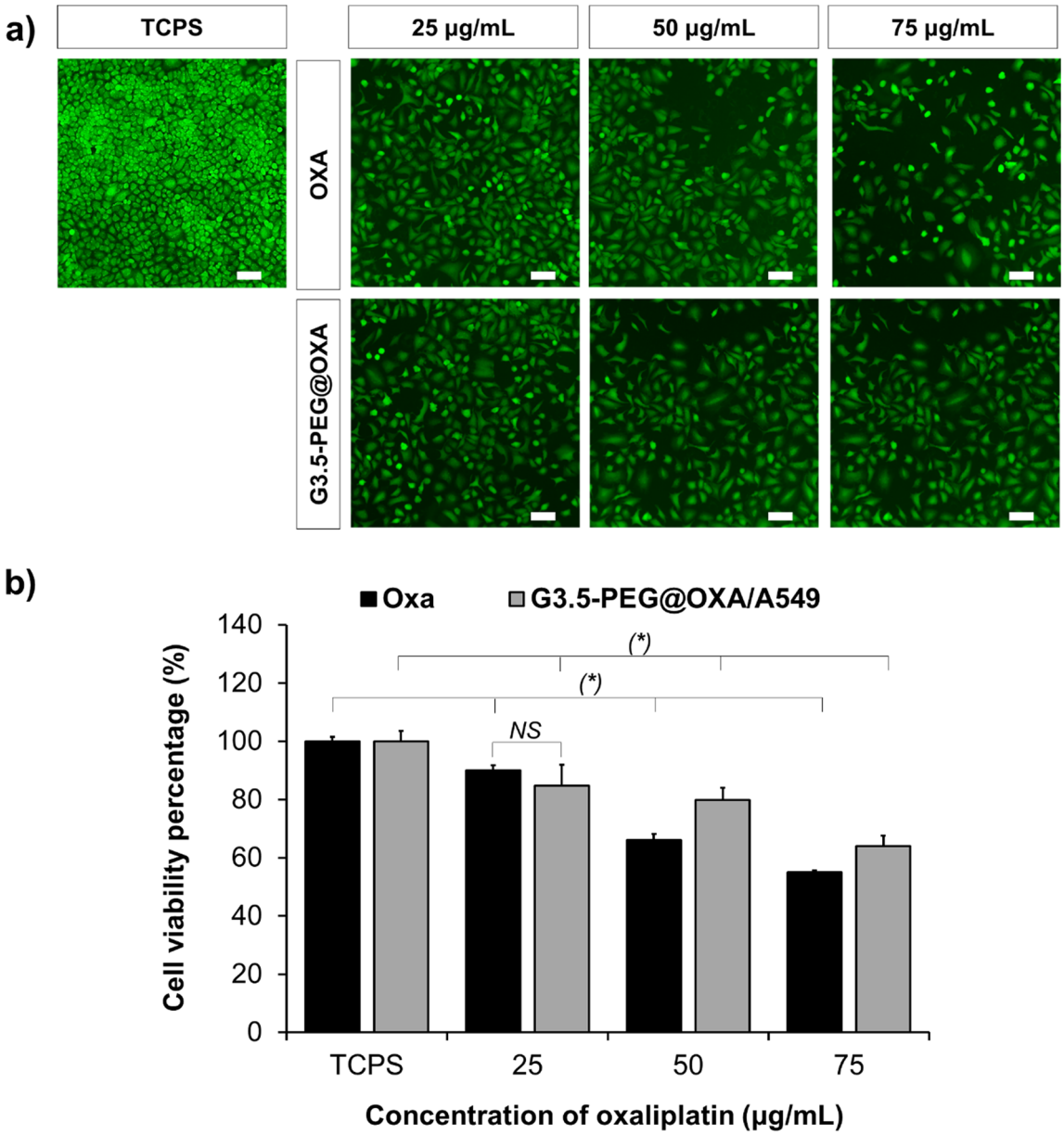

Fig. 8 A549 cells were stained by FDA/EB and observed by fluorescence microscopy after incubating with free OXA and G3.5-PEG@OXA for 48 h, TCPS was a control sample with the untreated A549 cells (**a**). The cell viability percentage of A549 cells compared to TCPS was performed by resazurin assay (**b**). Scale bar: 100 μm. (*) $P < 0.05$, *NS*: non-statistical difference

PAMAM dendrimer because the negative charge can avoid ionic interactions with cells and tissue surfaces [15]. In case of PEG, it is an inert synthetic polymer, uncharged and hydrophilic polymer that is a potential candidate to mask the surface of dendrimer to achieve good biocompatibility and circulation time [15]. Thus the G3.5-PEG were still able to achieve high cell viability (more than 100% compared to control sample) when the PEG content was increased from 4 to 32-fold per 1 dendrimer (Fig. 6b).

In vitro test of cancerous cell apoptosis

For an early studies, OXA was demonstrated its effective activity against colorectal cancer [9, 23]. In this study, to explore OXA's ability as well as OXA encapsulated in G3.5-PEG in another malignancies, three various lines of cancerous cells were utilized in this study. Human cervical cancer cells (HeLa), lung adenocarcinoma (A549), and breast cancer (MCF-7) were incubated with free OXA and G3.5-PEG@OXA at various OXA concentrations of 25, 50 and 75 μg/mL. Those cells were cultured on the tissue culture polystyrene plate in DMEM media that was a control and named as TCPS. After 48 h incubation, HeLa cells were washed with DPBS and then stained with FDA/EB reagents. Stained HeLa cells were imaged under a fluorescence microscope. The alive HeLa cells were indicated in green color, Fig. 7a showed that the alive HeLa density were decreased when increasing the concentration of both free OXA and

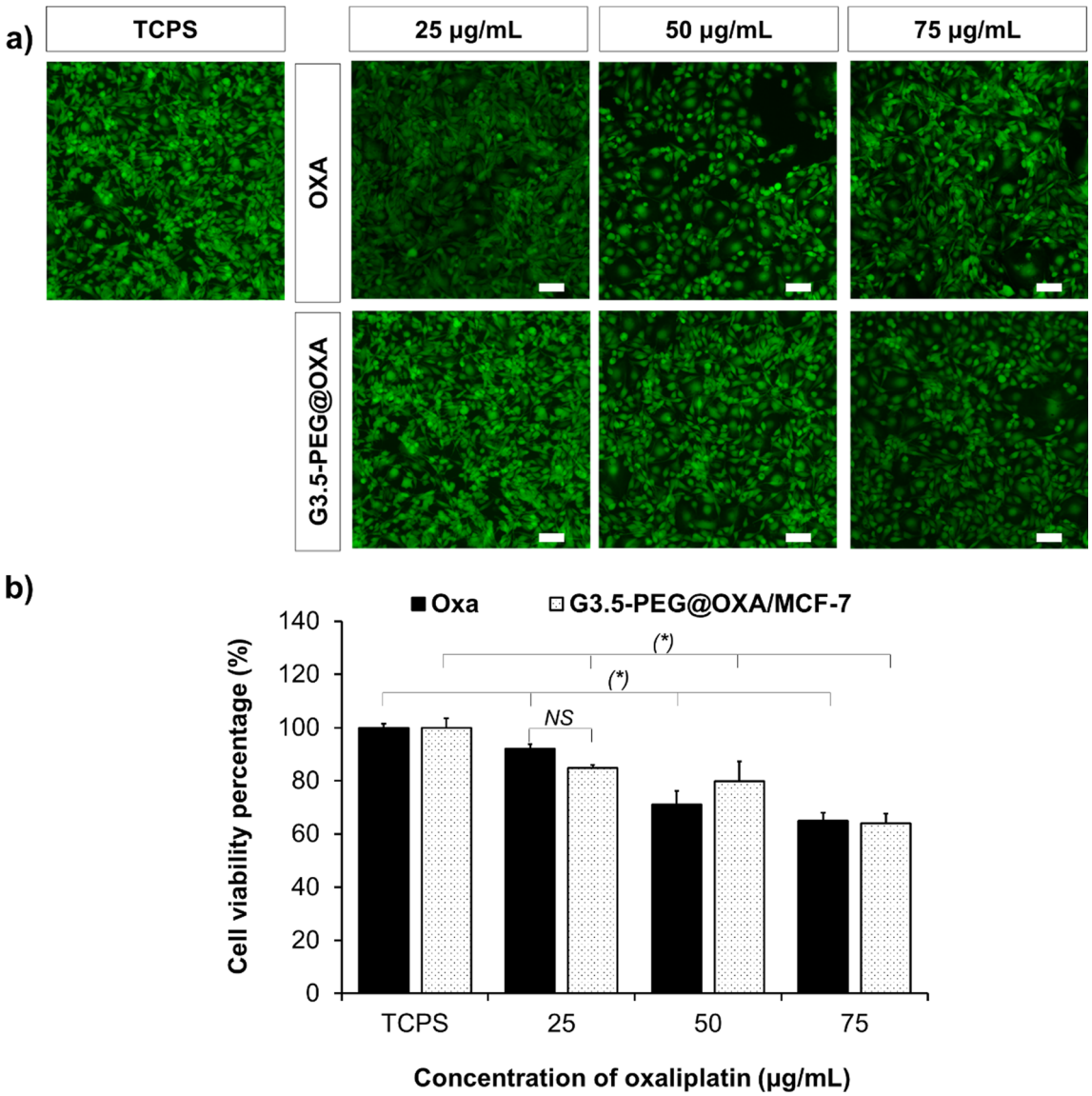

Fig. 9 MCF-7 cells were incubated with free OXA and G3.5-PEG@OXA for 48 h as a function of OXA content (TCPS (a control): MCF-7 cells without treatment). Then MCF-7 cells were stained with FDA/EB to be observed with fluorescent microscopy (**a**). MCF-7 viability percentage was calculated by using the OD data measured with resazurin assay (**b**). Scale bar: 100 μm. (*) $P < 0.05$, *NS*: non-statistical difference

G3.5-PEG@OXA. The dead HeLa cells were not appeared because of being washed out by DPBS. To investigate the cytotoxicity of this drug carrier system quantitatively, resazurin reagent was incubated with HeLa cells contacted free OXA and G3.5-PEG@OXA to record OD with microplate reader. The HeLa viability percentage was described at Fig. 7b. The viability of HeLa in pure DMEM media was put as 100%. With similar trend observed in alive cell images, the viability percentage of HeLa was significantly decreased in proportion to the increase of OXA concentration in both free type and carrier one. At low OXA concentration of 25 μg/mL, HeLa viability was around 90%, and the toxicity on HeLa cells between free OXA and G3.5-PEG@OXA was not different. At higher concentration of OXA from 50 μg/mL, free OXA exhibited higher toxicity than G3.5-PEG@OXA significantly. This phenomenon could be explained by the burst release of free OXA at first hour, while G3.5-PEG@OXA overcame this limitation and released the lower free OXA amount. Hence, viability percentage of HeLa in contacting with G3.5-PEG@OXA of 79.90% was higher than that contacting with free OXA of 69.00% when using same OXA concentration of 50 μg/mL. In case of increasing OXA concentration to 75 μg/mL, HeLa viability contacting G3.5-PEG@OXA and free OXA were decreased to 67.45% and 56.97% respectively. Although free OXA could kill HeLa cells quickly due to burst release, G3.5-PEG@OXA still showed much potential in clinical treatment because of preventing to lose OXA in blood stream, in plasma, and decrease of toxicity to normal cells.

Figures 8 and 9 showed the results of cell tests on A549 and MCF-7. For the A549 cells, following the OXA content of 25; 50 and 75 μg/mL, their corresponding viability percentages were obtained 84.80 ± 7.16; 79.90 ± 4.17 and 64.00 ± 5.57% (Fig. 8b). In case of the MCF-7 cells, the percentages of cell viability were 92.00 ± 1.55%; 71.00 ± 5.14% and 65.00 ± 3.00% when increasing OXA content in G3.5-PEG@OXA (Fig. 9b). The fluorescent images of A549 cells and MCF-7 were indicated in Figs. 8a and 9a respectively. The alive cells in green color demonstrated qualitatively about cell density in those samples. Observing qualitatively, the A549 and MCF-7 density were decreased following the increase of OXA content in G3.5-PEG nanoparticles that is consistent to the results of cell viability. However, the killing effects of OXA loaded in G3.5-PEG on three cell lines were not significantly different with free OXA. In spite of that, the G3.5-PEG@OXA still showed similar killing effect and will be exploited the advantages of PEGylation for further applications. When comparing between HeLa, A549 and MCF-7, G3.5-PEG@OXA displayed their activity better in HeLa cells that are also correspond to another study related to oxaliplatin cytotoxicity. Hela were more sensitive than A549 and MCF-7 when they were treated with OXA [24].

Conclusion

In conclusion, the G3.5-PEG was demonstrated as a cell compatibility materials for drug delivery applications. The G3.5-PEG could encapsulate OXA with high efficiency that exhibited by DLE of 75.69%. Its characteristics including nanoparticle sizes of less than 100 nm and non-charged nanoparticles were also suitable for drug carrier delivery in cancer treatment. The release kinetic of G3.5-PEG@OXA showed no burst release within first hours and continuously liberated OXA for next hours. Although free OXA still obtained the highest killing ability on HeLa cells, the G3.5-PEG@OXA could kill HeLa effectively and decreased the toxicity on normal cells in transportation within human body. The results of our study displayed that half-generation PAMAM dendrimers (G3.5) might be effective for the delivery of oxaliplatin with minimized side effects. For the future studies, the in vivo experiments should be performed to assess more the effectiveness of G3.5-PEG@OXA.

References

1. David A (2017) Peptide ligand-modified nanomedicines for targeting cells at the tumor microenvironment. Adv Drug Deliv Rev 119:120–142
2. Danhier F (2016) To exploit the tumor microenvironment: since the EPR effect fails in the clinic, what is the future of nanomedicine? J Control Release 244 (Pt A:108–121
3. Mintzer MA, Grinstaff MW (2011) Biomedical applications of dendrimers: a tutorial. Chem Soc Rev 40(1):173–190
4. Grabchev I, Staneva D, Vasileva-Tonkova E, Alexandrova R, Cangiotti M, Fattori A, Ottaviani MF (2017) Antimicrobial and anticancer activity of new poly(propyleneamine) metallodendrimers. J Polym Res 24(11):210
5. Svenson S, Tomalia DA (2005) Dendrimers in biomedical applications–reflections on the field. Adv Drug Deliv Rev 57(15): 2106–2129
6. D'Souza AA, Shegokar R (2016) Polyethylene glycol (PEG): a versatile polymer for pharmaceutical applications. Expert Opin Drug Deliv 13(9):1257–1275
7. Torchilin VP (1998) Polymer-coated long-circulating microparticulate pharmaceuticals. J Microencapsul 15(1):1–19
8. Baker DP, Lin EY, Lin K, Pellegrini M, Petter RC, Chen LL, Arduini RM, Brickelmaier M, Wen D, Hess DM, Chen L, Grant D, Whitty A, Gill A, Lindner DJ, Pepinsky RB (2006) N-terminally PEGylated human interferon-beta-1a with improved pharmacokinetic properties and in vivo efficacy in a melanoma angiogenesis model. Bioconjug Chem 17(1):179–188
9. Alcindor T, Beauger N (2011) Oxaliplatin: a review in the era of molecularly targeted therapy. Curr Oncol 18(1):18–25
10. Chen Y, Huang Z, Zhao H, Xu JF, Sun Z, Zhang X (2017) Supramolecular chemotherapy: cooperative enhancement of antitumor activity by combining controlled release of Oxaliplatin and consuming of Spermine by cucurbit[7]uril. ACS Appl Mater Interfaces 9(10):8602–8608
11. Thanh VM, Nguyen TH, Tran TV, Ngoc UP, Ho MN, Nguyen TT, Chau YNT, Le VT, Tran NQ, Nguyen CK, Nguyen DH (2018) Low systemic toxicity nanocarriers fabricated from heparin-mPEG and

PAMAM dendrimers for controlled drug release. Mater Sci Eng C Mater Biol Appl 82:291–298
12. Tummala S, Kumar MN, Pindiprolu SK (2016) Improved anti-tumor activity of oxaliplatin by encapsulating in anti-DR5 targeted gold nanoparticles. Drug Deliv 23(9):3505–3519
13. Forbes LM, O'Mahony AM, Sattayasamitsathit S, Wang J, Cha JN (2011) Polymer end-group mediated synthesis of well-defined catalytically active platinum nanoparticles. J Mater Chem 21(39):15788
14. Zhu S, Hong M, Tang G, Qian L, Lin J, Jiang Y, Pei Y (2010) Partly PEGylated polyamidoamine dendrimer for tumor-selective targeting of doxorubicin: the effects of PEGylation degree and drug conjugation style. Biomaterials 31(6):1360–1371
15. Kaminskas LM, Boyd BJ, Porter CJ (2011) Dendrimer pharmacokinetics: the effect of size, structure and surface characteristics on ADME properties. Nanomedicine 6(6):1063–1084
16. Yavuz B, Pehlivan SB, Unlu N (2013) Dendrimeric systems and their applications in ocular drug delivery. Sci World J 2013:732340
17. Osada K, Christie RJ, Kataoka K (2009) Polymeric micelles from poly(ethylene glycol)-poly(amino acid) block copolymer for drug and gene delivery. J Royal Soc Interface 3:S325–S339
18. Sawant S, Shegokar R (2014) Cancer research and therapy: where are we today? IJCTO 2(4):020408
19. Yellepeddi VK, Ghandehari H (2016) Poly(amido amine) dendrimers in oral delivery. Tissue Barriers 4(2):e1173773
20. Chen W, Tomalia DA, Thomas JL (2000) Unusual pH-dependent polarity changes in PAMAM dendrimers: evidence for pH-responsive conformational changes. Macromolecules 33(25): 9169–9172
21. Zhao Z, Lou S, Hu Y, Zhu J, Zhang C (2017) A Nano-in-Nano polymer-dendrimer nanoparticle-based Nanosystem for controlled multidrug delivery. Mol Pharm 14(8):2697–2710
22. Kang SJ, Durairaj C, Kompella UB, O'Brien JM, Grossniklaus HE (2009) Subconjunctival nanoparticle carboplatin in the treatment of murine retinoblastoma. Arch Ophthalmol 127(8):1043–1047
23. Patil AS, Gadad AP, Hiremath RD, Joshi SD (2018) Biocompatible tumor micro-environment responsive CS-g-PNIPAAm co-polymeric nanoparticles for targeted Oxaliplatin delivery. J Polym Res 25(3):77
24. William-Faltaos S, Rouillard D, Lechat P (2007) Cell cycle arrest by oxaliplatin on cancer cells. Fundam Clin Pharmacol 21(2): 165–172

Publisher's note Springer Nature remains neutral with regard to jurisdictional claims in published maps and institutional affiliations.